Relaxation dynamics of a single DNA molecule

E. Goshen,[1] W. Z. Zhao,[1,3] G. Carmon,[1] S. Rosen,[1] R. Granek,[2] and M. Feingold[1]
[1]*Department of Physics and The Ilse Katz Center for Nanotechnology, Ben Gurion University, Beer Sheva 84105, Israel*
[2]*Department of Biotechnology Engineering and Institute for Applied Biosciences, Ben Gurion University, Beer Sheva 84105, Israel*
[3]*Department of Mathematics, Capital Normal University, Beijing 100037, China*
(Received 3 February 2005; published 28 June 2005)

The relaxation of a single DNA molecule is studied. The experimental system consists of optical tweezers and a micron-sized bead that is tethered to the bottom of the sample by a single double-stranded DNA molecule. The bead slows down the DNA relaxation from a strongly stretched configuration such that it is passing through stretched equilibrium states. This allows for a theoretical description of the relaxation trajectory, which is in good agreement with experiment.

DOI: 10.1103/PhysRevE.71.061920 PACS number(s): 87.15.He, 36.20.Ey, 82.37.Rs

I. INTRODUCTION

Various biomolecules, e.g., actin, DNA, and microtubules, were found to be useful model systems for the study of polymers. These have been extensively investigated with the help of single-molecule manipulation techniques. In particular, the elastic behavior of DNA is one of the important aspects which has been addressed using a wide range of experimental methods, such as hydrodynamic drag, micropipettes, and optical and magnetic traps [1–5]. It is known that the elastic behavior of double-stranded DNA (dsDNA) is different in the various force regimes [6–11]. Based on the experimental results, several theoretical models have been proposed. Up to end-to-end extensions that are a few percent below the full contour length, L, the wormlike chain (WLC) model provides an accurate description for the elasticity of dsDNA [12–14]. In this model, the single dsDNA is regarded as a semiflexible chain which is characterized by its bending rigidity.

The dynamics and relaxation of DNA, on the other hand, has received less attention. Perkins *et al.* [1,16] studied the shape of relaxing DNA that was hydrodynamically stretched. A single DNA molecule was attached to a bead that was held in place by an optical trap and stretched by flow. When the flow is stopped, the DNA relaxes toward its coil configuration. Using fluorescently labeled DNA allowed them to monitor the conformational changes during relaxation. The dynamics of the free end follows an oscillatory trajectory with an amplitude that decays as the DNA coils up. In this case, the DNA dynamics is relatively fast and, therefore, takes place far away from stretched equilibria. Their results were interpreted by Brochard *et al.* [17–20] by considering the tension propagation and relaxation through the chain. Given a tension profile at a given instant, the configuration of the chain at this instant was conjectured using an extension of the Pincus blob model to nonuniform tensions. This extension has been previously invoked by these authors to interpret steady-state shapes of DNA in moderate flows [19,20]. The dynamics of DNA in shear flow was further studied by Doyle *et al.* [21].

Recently, Meiners and Quake [22] measured the thermal fluctuations of an extended single DNA using the femtonewton force spectroscopy technique. In their experiment, the two ends of a single DNA molecule were each attached to a bead and the DNA was stretched by a dual optical trap. The time correlations between the forces on the beads were measured in the highly stretched regime corresponding to extensions between $0.74L$ and $0.92L$. This was used to obtain the friction coefficient, spring constant, and relaxation time of the single extended DNA.

In another type of experiment, the relaxation dynamics of a DNA-bead complex was analyzed [23,24]. A single DNA molecule was attached to the bottom of the sample at one end and to a 3 μm bead at the other. Optical tweezers were used to stretch the DNA to extensions of up to $0.96L$. Turning off the trap allows the DNA to relax back to equilibrium. The bead allows us to monitor the motion of the end and, moreover, slows the dynamics to a time regime that is convenient for video microscopy. It also sets the dynamics in a range where the DNA passes through quasiequilibrium states. The dynamics of the bead is determined by the force of the DNA that acts against friction. It was found that a good fit to the data from the relaxation experiment can be obtained if one ignores the friction on the DNA. In fact, the absence of drag from the DNA is a direct consequence of the fact that the DNA is equilibrated.

It was recently pointed out that in such experiments it is crucial to properly take into account the influence of the neighboring surface on the dynamics of the DNA-bead complex [25]. In particular, the drag force on the bead depends on its height above the planar surface of the cover slip. Here, we present relaxation experiments where the initial conditions are high above the glass. Since the other end of the DNA is still attached to the glass, the relaxation occurs along a diagonal trajectory and the motion of the bead needs to be monitored both in the vertical direction and the horizontal plane. Similar experiments were recently preformed by Coelho Neto *et al.* In the experiments of Ref. [25], the height dynamics was not measured in the experiment but instead was deduced from the theoretical equation of motion. Our experiments improve on those of Ref. [25] by experimentally measuring the dynamics of the height during relaxation in addition to tracking the horizontal dynamics.

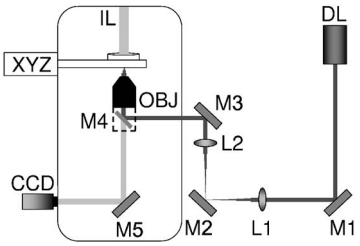

FIG. 1. The experimental setup: DL, diode laser; M1 to M5, mirrors (M4 is a dichroic mirror); L1,L2, lenses (telescope); OBJ, objective; XYZ, motorized XYZ stage; IL, white light illumination of the sample.

II. EXPERIMENTAL METHODS

We use double stranded DNA (dsDNA) from the λ phage (Promega) that is 16.5 μm long. The DNA is attached at one end to a polystyrene bead (Polysciences) and at the other end to the cover slip at the bottom of the sample. This is obtained using a low pH method [23,26]. In this protocol, we use 2.5 μl of plain polystyrene beads (2.5% solids in water), 5 μl DNA (530 μg/ml), and 330 μl PBS buffer (137 mM NaCl, 2.7 mM KCl, 10 mM Na_2HPO_4, 2 mM KH_2PO_4, and 0.8 mM NaN_3). The pH of the PBS was lowered to 6.0 using HCl. Coverslips for the sample are cleaned by sonication in toluene for 30 min. Beads, DNA, and buffer are mixed and incubated for 15 min at room temperature (RT) in a test tube. The sample consists of 30 μl solution between two coverslips that are kept apart by a parafilm ring. Once sealed, the sample is incubated for 60 min at RT before starting the experiment.

The low pH protocol is nonspecific, namely, it does not require a particular base pair sequence at the ends in order to obtain binding. As a consequence, shorter pieces of the DNA that break from the full λ-DNA due to pipetting are often found to tether beads to the bottom. Moreover, one also finds tethers that are longer than 16.5 μm. These are due to the hybridization of two λ-DNA's end to end. Also certain shorter pieces of λ-DNA can hybridize in the same manner. This hybridization occurs between the 12 base pairs single-stranded overhangs that are left at the end of the λ-DNA when it is cut from its native circular form. Since the overhangs at the different ends of the DNA are complementary, part of the DNA molecules will bind to others before they form the glass-DNA-bead complex. This leads to some variability in the lengths of the DNA tethers. We overcome this problem by directly measuring the length of the DNA. We do that by stretching the tether in four directions, namely left, right, up, and down, and determining the position of the corresponding escape point. Moreover, we determine the position of the tethering to the coverslip by averaging the Brownian motion that is performed by the bead-DNA complex when the trap is off. The length of the DNA results from the average distance between the tethering point and the escape points corrected using the force-extension formula [14].

The optical trap is obtained using a laser beam (SDL) focused through an 100× objective (Olympus UPlan Apo, 1.35NA, oil immersion) (see Fig. 1). Trapped beads are used to stretch the DNA to extensions that are close to L. Releasing the bead from the trap allows the DNA to relax back to its unstretched equilibrium configuration. We monitor this relaxation by tracking the bead at the end of the DNA. The tracking is done at video rate, 25 frames/s, and with single pixel resolution, 80 nm. Experiments were performed with two different bead sizes, namely diameters of $d_2=2.13\pm0.04$ μm and $d_3=2.79\pm0.14$ μm. The tweezers were adjusted to a maximal trapping force of 3.3 pN corresponding to a maximal extension, $z'_{0,max}$, of $z'_{0,max}=0.92$, where $z'=z/L$ and z is the end-to-end distance. The strength of the trap was calibrated using the Stokes force that acts on beads without DNA. Moving the sample at a fixed velocity relative to the trap, we determine the smallest velocity for which the bead is forced out of the trap due to the flow. In order to reduce the effect of the Brownian motion, each relaxation run was averaged over at least three different runs. We have verified that a single DNA molecule tethers the bead using the tweezers at maximal force to break the bead-DNA bond. Moreover, we found that the relaxation when more than one DNA is attached to the bead is significantly faster and can be clearly distinguished from the single DNA case.

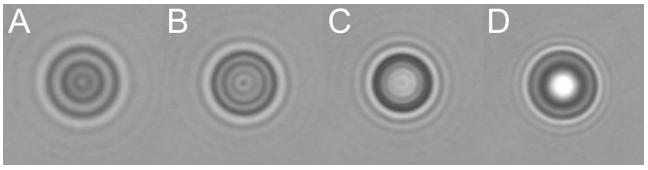

FIG. 2. Images of a d_3 bead at different heights from the focal plane. The image in D is closest to the focal plane. A, B, and C are 4.5 μm, 3 μm, and 1.5 μm, respectively, below D.

In order to avoid as much as possible the influence of the surface, we started the relaxation from a relatively large height above the coverslip. Such initial conditions are achieved using a trap that is raised from the glass by means of the telescope in the system (see Fig. 1). It consists of the L1 and L2 lenses that have equal focal length ($f=100$ mm) and are located at $2f+\epsilon$ from each other. While for $\epsilon=0$ the laser beam is unaffected by the telescope, for small, negative ϵ it becomes slightly divergent. As a result, the beam will be focused by the objective at a position slightly further than its focal plane, leading to a trap that is higher above the bottom of the sample. We track the dynamics of the bead using the interference rings method developed by Bensimon *et al.* As beads move away from the focal plane, their images develop interference rings that gradually grow larger. At the end of the relaxation experiment, the bead that was attached to the DNA is pulled free from the DNA-bead bond and attached to the glass surface. The same bead is used to build a library of images corresponding to different heights from the focal plane. The images in the library are obtained by raising the sample in equal steps of 0.3 μm (see Fig. 2). An interpolation algorithm is used to improve the height resolution down to 0.1 μm, comparable to the horizontal tracking resolution.

III. EQUATION OF MOTION

Turning off the trap after the DNA molecule has been stretched to z_0 starts the relaxation process. The presence of

the bead at the far end of the DNA simplifies its motion. First, it constrains the end of the DNA to move along a straight line aside from small fluctuations due to the Brownian motion of the bead. This way the stem and flower structures that were observed for free end DNA relaxation are avoided. Second, the bead slows down the relaxation. In the case of d_3 beads, it takes the DNA about 3 s (τ_R) to move from $z_0=0.90$ to $z=z_0/e=0.33$. This time scale is long compared to the longest relaxation time of a stretched chain [27],

$$\tau = \frac{4}{\pi \ln \frac{L}{\pi a}} \frac{\eta L^2}{f}, \tag{1}$$

where f is the force applied to the chain and a is the short length scale cutoff for dsDNA, $a=2$ nm. For forces in the range of 1 pN, which correspond to the initial conditions in our experiment, $\tau \sim 0.05$ s, while for forces of 0.1 pN corresponding to the end of the strong stretching regime, $z' \cong 0.5$, $\tau \sim 0.5$ s. Since $\tau \ll \tau_R$, one expects the motion of the DNA-bead system to be quasistatic for $z' > 0.5$. This allows us using equilibrium statistical mechanics to describe the dynamics in the large force regime.

During relaxation, the DNA-bead system moves under the influence of two forces: the force of the DNA on the bead, f, and the friction between the bead and the buffer, f_B. The inertia of the bead is six orders of magnitude smaller than f and can be neglected. Therefore, the equation of motion for the bead is

$$f = f_B. \tag{2}$$

In the limit of quasistatic dynamics and for $z' < 0.97$, the force due to the DNA on the bead is the equilibrium restoring force that is obtained from the the wormlike chain (WLC) model. A very good approximation to the WLC result is obtained from the interpolation formula of Marko and Siggia [14] including the corrections due to Bouchiat *et al.* [15],

$$f(z') = \frac{kT}{A}\left(z' + \frac{1}{4(1-z')^2} - \frac{1}{4} + \sum_{i=2}^{7} \alpha_i (z')^i \right), \tag{3}$$

where A is the persistence length, $\alpha_2 = -0.516\,422\,8$, $\alpha_3 = -2.737\,418$, $\alpha_4 = 16.074\,97$, $\alpha_5 = -38.876\,07$, $\alpha_6 = 39.499\,44$, and $\alpha_7 = -14.177\,18$. At this point, one might naively expect that there should be an additional contribution to the force equation due to the friction between the DNA and the buffer. However, this contribution vanishes in the quasistatic limit. This was explicitly shown in previous work [27], where the full wormlike chain dynamics of the DNA-bead system was considered. Qualitatively, this is because the friction between DNA and fluid limits the rate at which the DNA modes decay. If the dynamics occurs on a time scale much slower than the equilibration time, the modes represent fast variables that have been integrated out and along with them also the influence of the viscosity on the dynamics of the DNA.

The flow around the moving bead is in the Stokes regime such that, far away from boundaries, $f_B = 6\pi\eta r_i v_z$, where η is the viscosity of the buffer, $r_i = d_i/2$ is the radius of the bead, and $v_z = dz/dt$ is its velocity. This friction is enhanced in the vicinity of a flat surface. In order to minimize the effect of the glass surface, we use initial conditions that are at some height, h, above the surface (see Fig. 3). A diagonal trajectory is obtained since the other end of the DNA is attached to the surface. The Stokes friction coefficient, γ, is anisotropic near an infinite surface,

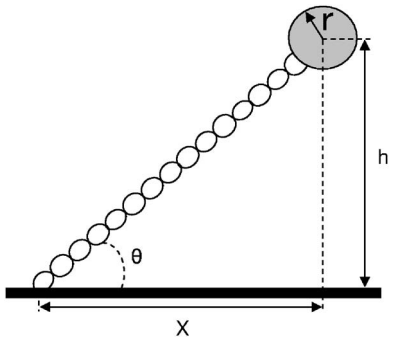

FIG. 3. Schematic view of the glass-DNA-bead complex.

$$\gamma_{\parallel} \cong \frac{6\pi\eta r}{\left[1 - \frac{9}{16}\left(\frac{r}{h}\right) + \frac{1}{8}\left(\frac{r}{h}\right)^3 - \frac{45}{254}\left(\frac{r}{h}\right)^4 - \frac{1}{16}\left(\frac{r}{h}\right)^5\right]}, \tag{4}$$

$$\gamma_{\perp} \cong 6\pi\eta r\left(1 + \frac{r}{h-r}\right), \tag{5}$$

where $\gamma_{\parallel}$ and $\gamma_{\perp}$ are the friction coefficients in the direction parallel and perpendicular to the surface, respectively [28–30]. The accuracy of Eq. (4) is better than 0.1% and that of Eq. (5) is on average 4% in the range relevant to our experiments.

From Eq. (2), we obtain the equations of motion for the bead dynamics,

$$\gamma_{\parallel}\dot{z}_{\parallel} = f(z)\cos\theta, \tag{6}$$

$$\gamma_{\perp}\dot{z}_{\perp} = f(z)\sin\theta, \tag{7}$$

where $\sin\theta = h/(z+r)$ (see Fig. 3).

IV. EXPERIMENTAL RESULTS

In order to understand the properties of the DNA relaxation, we study the effect of changing the parameters of the experiment. We vary three parameters, namely the initial conditions, the length of the DNA, L, and the size of the bead, r. We find that the variation of these three parameters leads to simple changes in the trajectory, $z(t)$, that can be accounted for by rescaling the time. The scaling behavior of $z(t)$ indicates which are the dominating terms in the equation of motion for the DNA-bead construct. Whenever the relaxation dynamics brings the bead to lower heights, $h \lesssim 3.5$ μm, the glass surface and the excess of DNA that is attached to it modify the dynamics in a complicated way. For this reason, we restrict our study to the short-time regime, corresponding to high tensions, $z/L > 0.5$.

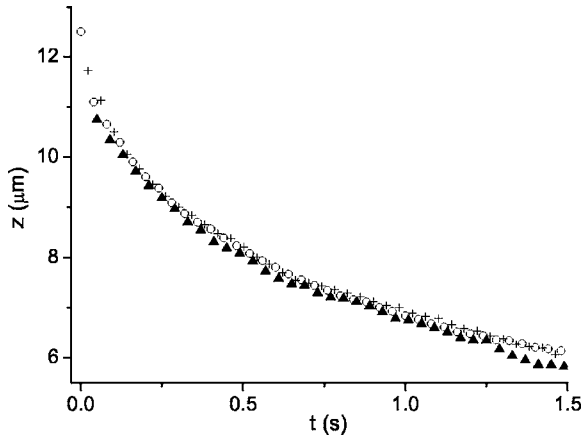

FIG. 4. Three relaxation trajectories that were measured for the same DNA-bead complex only with the different initial conditions. Here we use DNA with $L=13.9$ μm, d_3 beads, and $h_0=6.1$ μm. The different initial conditions are $z_0=12.5$ μm (open circles), 11.7 μm (crosses), and 10.8 μm (triangles).

The effect of varying the initial condition, z_0, is illustrated in Fig. 4. We find that the trajectories corresponding to different z_0 become equivalent within the experimental error if the time axis is shifted by an appropriate constant, $G(z_0)$. This constant corresponds to the time it takes the bead to move from the largest z_0, $z_0=0.9L$, to the z_0 of each particular trajectory. This behavior indicates that $z(t)$ is the solution of a first-order differential equation. It also supports the claim that during relaxation, the DNA is passing through quasiequilibrium intermediate states that do not depend on the history of the motion.

Changing all three parameters, namely L, r, and the initial conditions, leads to apparently different trajectories. In Fig. 5(a), we show four such trajectories that, in contrast to Fig. 4, have no common parameters aside from z_0/L. However, a simple rescaling of the axes such that $z'=z/L$ is plotted versus $t'=t/t_0$, where $t_0=6\pi\eta ALr/kT$, leads to the collapse of the trajectories onto a single function [see Fig. 5(b), the differences between the four curves are smaller than the experimental error]. This scaling is also found to hold almost exactly in the corresponding numerical solution of the theoretical equations of motion, Eqs. (6) and (7) [see Fig. 5(c)]. In fact, this scaling is exact if the relaxation geometry is such that h is constant, that is, it takes place parallel to the glass surface. Since in our experiment h is about three times smaller than L, the breaking of scaling due to the anisotropy of the friction coefficient is negligible.

The picture emerging from the experiments in Figs. 4 and 5 is that to a good approximation the variation of the parameters can be accounted for either by using rescaled variables, $z'(t')$, or by shifting the time. Next we compare the experimental trajectories with the theory of Eqs. (6) and (7) for a particular set of parameters. For a DNA molecule of $L=13.91$ μm and a bead of diameter d_3, we use an individual trajectory that starts from $z_0'=0.85$ and $h_0=6.1$ μm to compare to theory (see Fig. 6). In the short-time regime, we find good agreement between experiment and theory for the time evolution of both z' and h. The large errors in the height measurement, up to 6%, are mostly due to the inaccuracy of

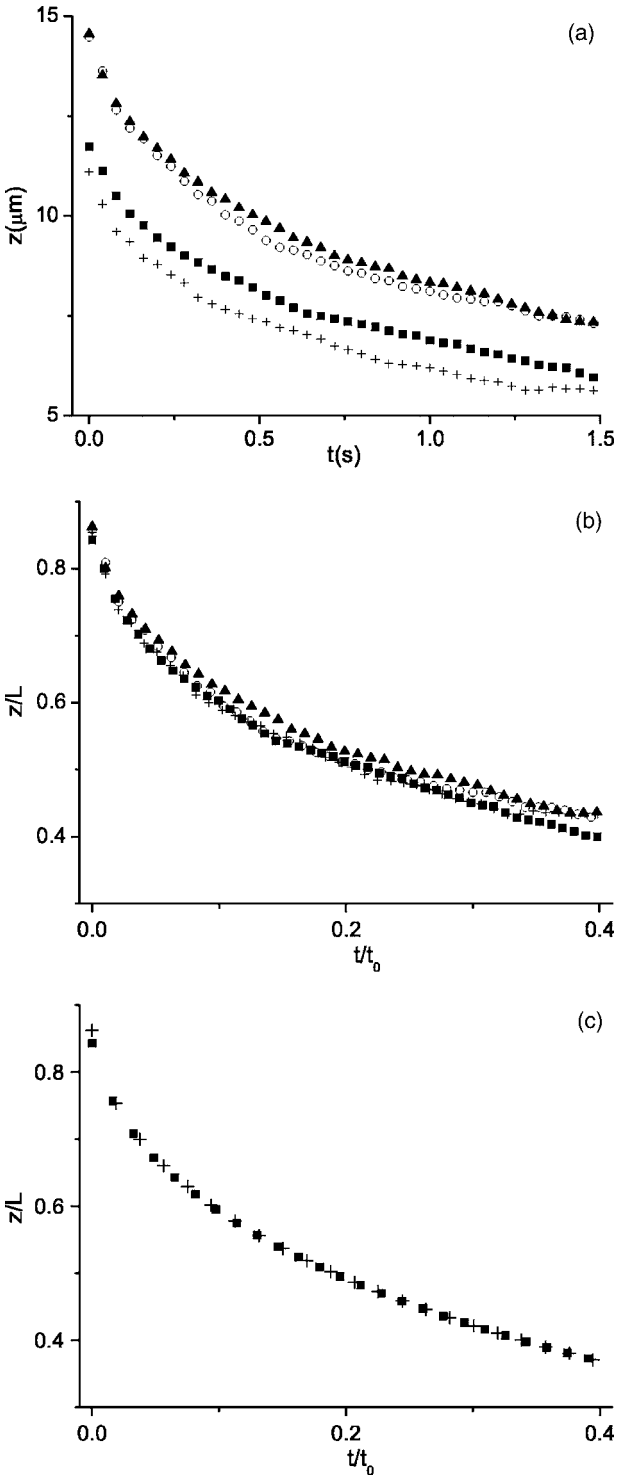

FIG. 5. Dependence of the relaxation trajectories on the various parameters. (a) Four trajectories that have the same $z_0'=0.85\pm0.01$ are shown: T_1 (triangles), T_2 (open circles), T_3 (squares), and T_4 (crosses), such that for T_1, $L=16.9$ μm, d_2 bead, $h_0=4.5$ μm; for T_2, $L=16.9$ μm, d_2 bead, $h_0=4.6$ μm; for T_3, $L=13.9$ μm, d_3 bead, $h_0=6.3$ μm; and for T_4, $L=13.0$ μm, d_3 bead, $h_0=5.5$ μm. Each trajectory is averaged over at least three runs in order to reduce Brownian fluctuations. (b) The same as in (a) only with rescaled axes. (c) The theoretical trajectories corresponding to the initial conditions of T_1 (plus) and T_3 (squares).

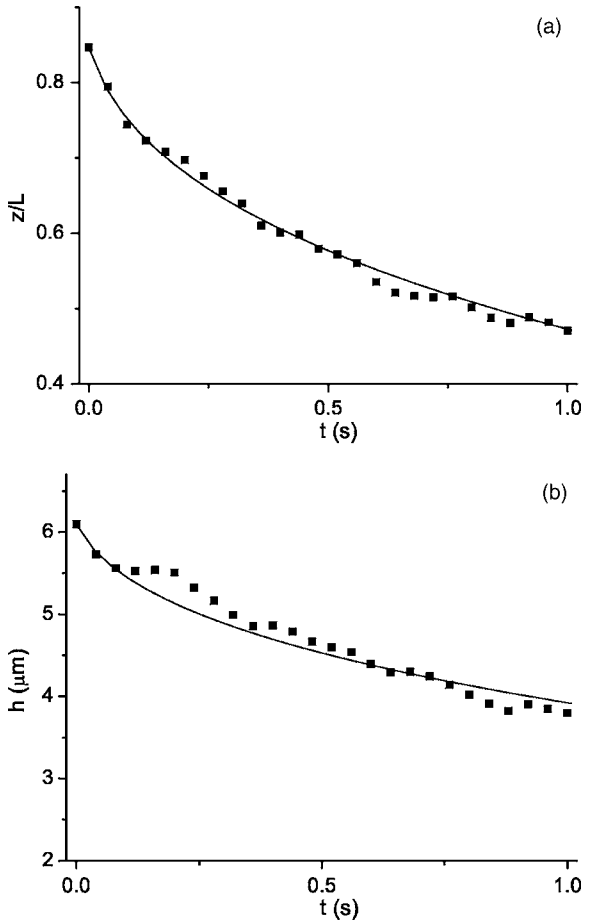

FIG. 6. Comparison between theory (full line) and experiment (squares) for one of the trajectories of Fig. 5, T_3 (single run). For the theory, we used $A=50$ nm and $\eta=0.98$ m Ps (there are no free parameters). (a) Comparing the measured trajectory (squares) to theory (line). The experimental error is at most 4%. (b) Comparing the measured height (squares) to theory (line). The largest experimental error is about 6%.

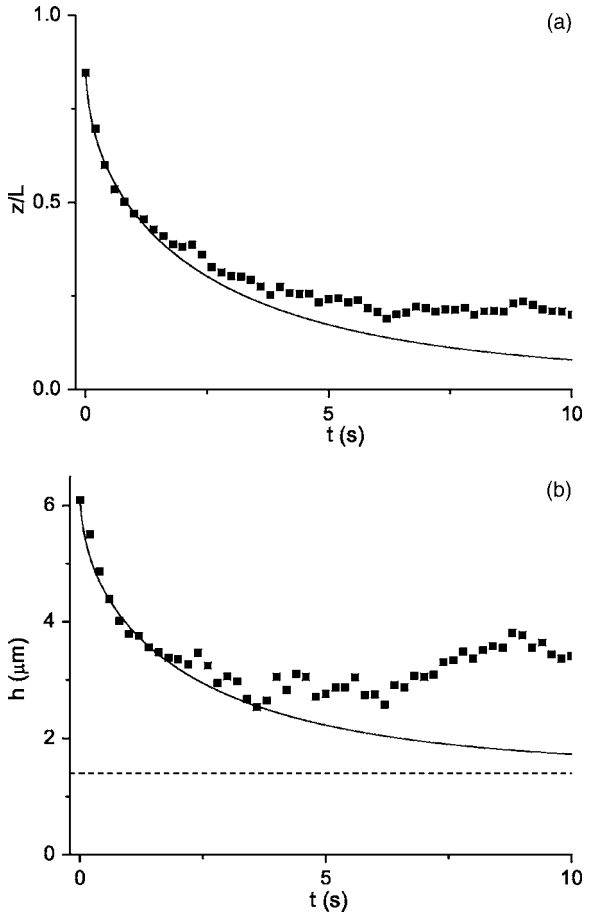

FIG. 7. Same as in Fig. 6 only here the long-time regime is also shown, $t<10$ s. For clarity, not all data points are displayed (only one every five points). (a) Comparing the measured trajectory (squares) to theory (line). (b) Comparing the measured height (squares) to theory (full line). The dashed line marks the radius of the bead.

the 0.3 μm motor steps used to build the library of defocused bead images (Fig. 2). It should be noted that in addition to the measurement errors, deviations between the theory and experiment are also due to the random Brownian motion that is not taken into account in Eqs. (6) and (7). In other words, one possible reason for the deviation of the data points from the theoretical prediction is random thermal forces acting on the chain and controlling the dynamics of its undulations, and on the bead itself. However, in view of the long correlation time for the apparent noise, 0.2–0.3 s, relative to the longest mode relaxation time estimated above, $\tau\sim 0.05$ s, this seems unlikely. Instead, these deviations could be due to the failure of the quasistatic description, as discussed in Ref. [27]. Nonetheless, accounting for the additional friction due to the glass surface is crucial for obtaining this approximate agreement.

For larger times, $t\gtrsim 1$ s, when the relaxation dynamics of the DNA brings the bead close to the glass surface, $h \lesssim 3.5$ μm, the agreement between theory and experiment is lost (see Fig. 7). At about this point, the measured height does not decrease any further while the dynamics predicted by Eqs. (6) and (7) continues to approach the bottom of the sample. This is not surprising considering that the excluded volume of the folding DNA molecule was not taken into account in Eqs. (6) and (7). The bead radius together with the gyration radius of the DNA, r_G, limit the approach of the bead center to the glass. In fact, in the equilibrium configuration the folded DNA induces an effective repulsion between the bead and the glass surface. This repulsion is of entropic origin and can be estimated by approximating the bead as a second planar surface [31]. This gives an equilibrium height of $h_T=2.6$ μm for the parameters of Fig. 7. The approximation in this calculation is such that h_T overestimates the exact result. Experimentally, however, we find that in equilibrium the bead fluctuates at a larger average height of $h_e=3.6\pm 0.2$ μm. The origin of this enhanced repulsion from the glass surface is presently not clear.

V. CONCLUSIONS

We have shown that the relaxation dynamics of a single DNA molecule that is attached to a micron-sized bead can be

approximately described using quasistatic dynamics if the influence of the neighboring surface is properly accounted for. Complications due to the surface limit our description to the short-time regime. As was shown in Ref. [25], this dynamics can be used to measure the persistence length of the DNA, A. This method is much simpler than the standard approach that requires measuring the force-extension curve, $f(z)$.

Some discrepancies do remain between this theoretical description and experiment, and it is possible that these are due to the failure of the quasistatic approach. This implies that undulations do not have sufficient time to recover equilibrium statistics at each extension, as the extension changes from one value to the next. The latter, nonequilibrium, effect has been accounted for in Ref. [27], however, without accounting for the nearby surface. It would be worthwhile to extend the DNA relaxation experiments to regimes where the quasistatic picture fails completely [27]. This can be achieved either by using smaller beads, $r \lesssim 0.1$ μm, or by measuring at shorter time scales, $t \lesssim 1$ ms. In this very short-time regime, the tension propagation along the DNA will also have to be incorporated in the description of the dynamics.

ACKNOWLEDGMENTS

We thank R. Amit, D. Bensimon, V. Croquette, M. Elbaum, O. Krichevsky, O.N. Mesquita, and S. Vanounou for useful discussions and suggestions. This research was supported in part by the Israel Academy of Science and Humanities (Grant No. 263/00).

[1] T. T. Perkins, D. E. Smith, R. G. Larson, and S. Chu, Science **268**, 83 (1995).
[2] P. Cluzel, A. Lebrun, C. Heller, R. Lavery, J.-L. Viovy, D. Chatenay, and F. Caron, Science **221**, 792 (1996).
[3] S. B. Smith, Y. Cui, and C. Bustamante, Science **271**, 795 (1996).
[4] R. M. Simmons, J. T. Finer, S. Chu, and J. Spudich, Biophys. J. **70**, 1813 (1996).
[5] M. D. Wang, H. Yin, R. Landick, J. Gelles, and S. M. Block, Biophys. J. **72**, 1335 (1997).
[6] P. Cluzel, A. Lebrun, C. Heller, R. Lavery, J. L. Viovy, D. Chatenay, and F. Caron, Science **271**, 792 (1996).
[7] S. B. Smith, Y. Cui, and C. Bustamante, Science **271**, 795 (1996); S. B. Smith, Y. Cui, A. C. Hausrath, and C. Bustamante, Biophys. J. **68**, A250 (1995).
[8] P. Cizeau and J.-L. Viovy, Biopolymers **42**, 383 (1997).
[9] A. Ahsan, J. Rudnick, and R. Bruinsma, Biophys. J. **74**, 132 (1998).
[10] M. Grandbois, M. Beyer, M. Rief, H. Clausen-Schaumann, and H. E. Gaub, Science **283**, 1727 (1999).
[11] D. Bensimon, A. J. Simon, V. Croquette, and A. Bensimon, Phys. Rev. Lett. **74**, 4754 (1995).
[12] C. Bustamante, J. F. Marko, S. B. Smith, and E. D. Siggia, Science **265**, 1599 (1994).
[13] A. Vologodskii, Macromolecules **27**, 5623 (1994).
[14] J. F. Marko and E. D. Siggia, Macromolecules **28**, 8759 (1995).
[15] C. Bouchiat, M. D. Wang, J.-F. Allemand, T. Strick, S. M. Block, and V. Croquette, Biophys. J. **76**, 409 (1999).
[16] T. T. Perkins, S. R. Quake, D. E. Smith, and S. Chu, Science **264**, 822 (1994).
[17] F. Brochard-Wyart, Europhys. Lett. **23**, 105 (1993).
[18] F. Brochard-Wyart, H. Hervet, and P. Pincus, Europhys. Lett. **26**, 511 (1994).
[19] F. Brochard-Wyart, Europhys. Lett. **30**, 387 (1995).
[20] S. Manneville, P. Cluzel, J.-L. Viovy, D. Chatenay, and F. Caron, Europhys. Lett. **36**, 413 (1996).
[21] P. S. Doyle, B. Ladoux, and J. L. Viovy, Phys. Rev. Lett. **84**, 4769 (2000).
[22] J.-C. Meiners and S. R. Quake, Phys. Rev. Lett. **84**, 5014 (2000).
[23] G. V. Shivashankar, M. Feingold, O. Krichevsky, and A. Libchaber, Proc. Natl. Acad. Sci. U.S.A. **96**, 7916 (1999).
[24] M. Feingold, Physica E (Amsterdam) **9**, 616 (2001).
[25] J. C. Neto, R. Dickman, and O. N. Mesquita, Physica A **345**, 173 (2005).
[26] J. F. Allemand, D. Bensimon, L. Jullien, A. Bensimon, and V. Croquette, Biophys. J. **73**, 2064 (1997).
[27] Y. Bohbot-Raviv, W. Z. Zhao, M. Feingold, C. H. Wiggins, and R. Granek, Phys. Rev. Lett. **92**, 098101 (2004).
[28] H. Faxen, Ark. Mat., Astron. Fys. **18**, 1 (1924).
[29] H. Brenner, Chem. Eng. Sci. **16**, 242 (1961).
[30] A. J. Goldman, R. G. Cox, and H. Brenner, Chem. Eng. Sci. **22**, 637 (1967).
[31] R. Granek (unpublished). The calculation uses the propagator for the Gaussian chain in a box. See M. Doi and S. F. Edwards, *The Theory of Polymer Dynamics* (Clarendon Press, Oxford, 1986).